

# The direct assimilation in the ECMWF 4D-Var system of principal component scores derived from shortwave IASI spectra

Marco Matricardi, Tony McNally

ECMWF, Shinfield Park, Reading, RG2 9AX, UK

## Abstract

A principal component based version of the RTTOV fast radiative transfer model has been implemented into the ECMWF assimilation system to study the direct assimilation of principal component scores derived from IASI spectra. We have carried out extensive trials by conveying to the analysis system information in the form of principal component scores and radiances from band 3 of the IASI spectrum. We have performed a detailed study of the analysis increments in temperature for the two systems and have assessed the relative impact on forecast scores. Our study shows that information from the IASI spectrum can be efficiently communicated to the analysis by the direct assimilation of principal component scores.

## 1 INTRODUCTION

The operational use of IASI radiances (Collard and McNally 2008) at the European Centre for Medium-Range Weather Forecasts (ECMWF) is currently restricted to a selection of temperature sounding channels in the long-wave region of the spectrum and to a very limited number of humidity sounding channels in the main infrared water vapour band. The short-wave spectral region covered by IASI band-3 (2000-2760  $\text{cm}^{-1}$ ) contains excellent temperature sounding channels which could also be exploited for assimilation into a Numerical Weather Prediction (NWP) system. Channels in the IASI short-wave band are currently underused compared to similar channels in the long-wave region for a number of reasons, which include cloud detection and radiative transfer biases, day-night variations in data usability due to non-local thermodynamic equilibrium (LTE) and solar effects, increased instrument noise. All these issues are under investigation with the aim of optimizing the use of the data.

Regarding the increased instrument noise, as discussed in Antonelli et al. (2004), the use of principal component analysis (PCA) can remove a significant fraction of the uncorrelated random error present in the observations. Based on PCA noise filtering, we are studying the feasibility of mitigating the instrument noise problem in IASI band-3 through the direct assimilation of principal components (PC) scores. The direct use of PCs in an NWP assimilation system has required the development of the PC\_RTTOV (Matricardi 2010) fast radiative transfer (RT) model which can efficiently simulate PC scores given first-guess fields of temperature, water vapour, ozone, and, surface properties. In this study, PC\_RTTOV is used to simulate PC scores derived from a subset of 297 IASI channels between 2200  $\text{cm}^{-1}$  and 2520  $\text{cm}^{-1}$ .

## 2 THE SELECTION OF THE SHORT-WAVE CHANNELS USED IN THE ASSIMILATION TRIALS

Because a large number of channels in IASI band-3 are characterized by very high values of the instrument noise, channels in IASI band-3 are ideal candidates for the use in preliminary trials aimed at assessing the merits of the direct assimilation of PC scores into a NWP system. PCA should in fact remove a significant fraction of the uncorrelated random noise present in the observations by

exploiting the high level of correlation between the channels of high-resolution infrared sounders like IASI.

The selection of a subset of channels within IASI band-3 has been guided by the assumption that the best channels are those that are sensitive to absorption due to single gas species. The absorption features in IASI band-3 are due mainly to H<sub>2</sub>O, O<sub>3</sub>, CO<sub>2</sub>, N<sub>2</sub>O, CO and CH<sub>4</sub>. Because the main intent of this paper is temperature sounding, we have isolated channels contaminated only by CO<sub>2</sub> and N<sub>2</sub>O whose concentrations are close to constant in space and time.

For the inference of temperature profiles we have selected channels that are located in spectral regions characterized by narrow weighting functions because this would improve the vertical resolution of the temperature profiles. Channels with sharp weighting functions are typically located between absorption lines (Kaplan et al. 1977) where the absorption coefficient increases with pressure. The exclusive use of these channels, however, would not allow the sounding of the upper region of the atmosphere because the absorption in the wings of the lines is weaker than the absorption in the centre of the lines and channels between lines can only see lower in the atmosphere. To cover the upper regions of the atmosphere, channels between lines must be supplemented by channels located on top of lines. Based on these criteria, we have selected the set of 297 channels (hereafter denoted as the B3\_OP set) represented by the red dots in Figure 1 (the black curve is a typical spectrum for the whole IASI band-3). Note that, because the same set of channels is going to be used in conventional radiance assimilation trials, we have oversampled channels located in the noisiest regions of the spectrum. The region between 2380 and 2400 cm<sup>-1</sup> (the head of the R-branch of the  $\nu_3$  CO<sub>2</sub> band) merits special mention because these lower tropospheric sounding channels have the sharpest possible weighting functions of any part of the infrared spectrum.

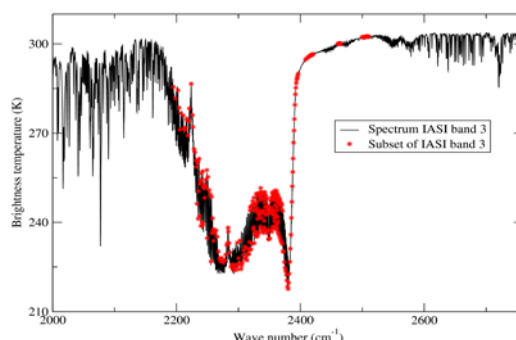


**Figure 1:** The IASI band-3 spectrum showing the channels selected for use in the short wave assimilation trials.

We should note that although the widths of the weighting functions are a useful measure of the vertical resolution of radiance measurements, the curves that represent the vertical resolving power are better characterized by the integrand in the radiative transfer equation, i.e. the Planck function,  $B$ , times the weighting function,  $W$ . Because in the short wave the Planck function depends strongly on temperature, this makes the short wave radiances much less sensitive to the temperatures in the coldest regions of the atmosphere (e.g. the tropopause) than the corresponding radiances in the long wave region of the spectrum.

### 3 THE DESIGN OF THE PC ASSIMILATION SYSTEM

The methodology of direct PC score assimilation is shown schematically in Figure 2. The observed IASI spectra are first screened for the presence of cloud and contaminated spectra are discarded. This must be done before assimilation as the PC training has been performed with only completely clear data and none of the eigenvectors correspond to cloud signals. The clear spectra are then projected on to the chosen PC basis (in this case derived from the  $N=297$  selected channels of IASI band-3) to

produce vectors of observed PC scores  $\mathbf{Y}_{OBS}^{PC}$ . In principle each vector of observed PC scores has length  $N$ , but in practice we chose to assimilate only the first  $M$  of these (where  $M < N$  in ranked order). In truncating the vector of observed PC scores we aim to retain the low order modes (rank 1,2,3 .. $M$ ) that convey information about the atmospheric state and discard higher order eigenvectors that convey information about noise in the observed spectrum. To determine the optimal number of PC scores we have carried out assimilation trials where we have changed the number of PC scores. The final number of  $M=10$  PC scores has been selected based on the improvements in the fit of temperature background and analysis profiles to radiosonde observations.

## PC analysis system design

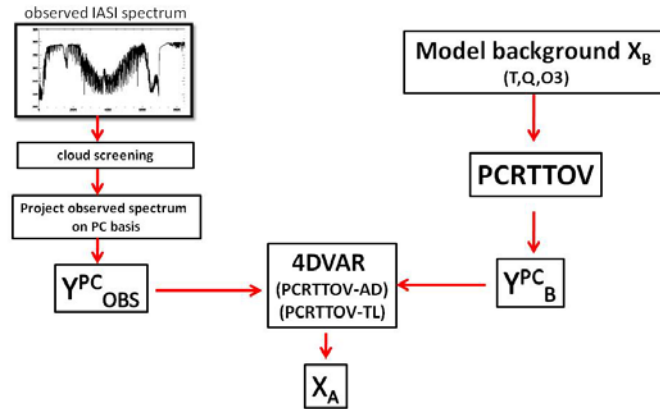


**Figure 2:** The methodology of the direct PC score assimilation system

The observed  $M$  PC scores are provided as input to the 4D-Var. In here, estimates of the atmospheric state ( $X$ ) are used to simulate model equivalents of the  $M$  PC scores  $\mathbf{Y}^{PC}(X)$  using the radiative transfer model PC\_RTTOV as the observation operator. If we ignore the time integration of the forecast model to the observations the cost function to be minimized is essentially:

$$J(\mathbf{X}) = [\mathbf{X} - \mathbf{X}_B]^T \mathbf{B}^{-1} [\mathbf{X} - \mathbf{X}_B] + [\mathbf{Y}_{OBS}^{PC} - \mathbf{Y}^{PC}(X)]^T \mathbf{R}^{-1} [\mathbf{Y}_{OBS}^{PC} - \mathbf{Y}^{PC}(X)] \quad (1)$$

where the accuracy of the background estimate of the atmospheric state  $\mathbf{X}_B$  is described by the error covariance  $\mathbf{B}$  and the accuracy of the observations and associated observation operator is described by the error covariance  $\mathbf{R}$ . The background error covariance  $\mathbf{B}$  used in this study is identical to that from the operational ECMWF assimilation system. The atmospheric state  $\mathbf{X}_A$  that minimizes the above cost function is referred to as the analysis and the departures of this from the background atmospheric state  $\mathbf{X}_B$  are referred to as analysis increments.

To specify the elements of  $\mathbf{R}$  we have accumulated a statistics of the PC score departures by monitoring the observed and background PC scores over a period of four weeks using sea-surface and nighttime observations, the latter to avoid non-local thermodynamic equilibrium (LTE) and solar effects. As statistics of these departures contain an additional contribution from the error in the background state – they may be regarded as an upper bound upon the combined observation and forward model error. The standard deviation of the departures for the first 10 PC scores are tabulated in Table 1.

PC Number	Standard deviation
1	8.496071
2	3.148550
3	4.296503
4	2.031785
5	1.438960
6	1.338933
7	1.660405
8	1.299309
9	1.191461

10	1.156676
----	----------

**Table 1. The standard deviation of the PC scores background departures.**

Note that these results have been obtained using first-guess fields from the operational analysis. To finely tune the elements of  $\mathbf{R}$  we have carried out assimilation trials where, as for the determination of the optimal number of PC scores, we have varied the elements of  $\mathbf{R}$  and have looked at the improvements in the fit of temperature background and analysis profiles to radiosonde observations. Based on these trials, the elements of  $\mathbf{R}$  have a value that is equal to 0.35 times the value of the standard deviation of the background departures.

## 4 THE IMPACT OF IASI PC SCORES ON ANALYSES AND FORECASTS

To test the impact of the IASI PC scores on the assimilation system, we have designed four assimilation experiments that consist of a baseline experiment, two reference experiments and a PC score experiment. The baseline experiment (hereafter referred to as the NOSAT experiment) uses only conventional data. The first reference experiment (hereafter referred to as the B1 experiment) uses conventional data and the IASI operational long wave radiances whereas the second reference experiment (hereafter referred to as the B3\_OP experiment) uses conventional data and the short wave IASI radiances selected in this paper. Finally, the PC score experiment (hereafter referred to as the B3\_OP\_PC experiment) uses conventional data and PC scores derived from the short wave IASI radiances used in the B3\_OP experiment. In the PC score assimilation experiment we have introduced a PC based quality control for residual clouds (Matricardi and McNally 2011). The correction of biases in the PC score departures is carried out using the operational Variational Bias Correction (VarBC) scheme (Dee, 2004) currently in use at ECMWF. The experiments have been run using a reduced resolution version (T511) of the ECMWF IFS cycle 36R1 (T799) completing a month of testing from 12 June 2010 to 15 July 2010. For consistency reasons, all the relevant experiments use the same cloud detection scheme (i.e. the FOV based cloud detection scheme described by Matricardi and McNally (2011) and assimilate only high-time radiance data to avoid any solar and non-LTE contamination in the short-wave region of the spectrum. In the PC score experiment, we have conservatively blacklisted all the data over sea-ice because in a few instances, preliminary very low-resolution experiments have shown unreasonable analysis increments. The origin of this behavior is still under investigation. Finally, we should stress that, due to the time constraints of the study, the tuning of the IASI band 3 radiance assimilation experiment has received far less attention than the IASI band 3 PC score assimilation experiment. For instance, we could not spare any resources for the tuning of the observation errors. Consequently, we have used values equal to the standard deviation of the departures between observed and simulated radiance spectra.

### 4.1 The analysis increments and the fit to radiosonde data

Figure 3 shows the globally averaged mean and root-mean-square temperature analysis increments evaluated over one month of assimilation. Results for the reference IASI long wave experiment (B1) are in black while results of the IASI short wave PC score experiment (B3\_OP\_PC) are in red.

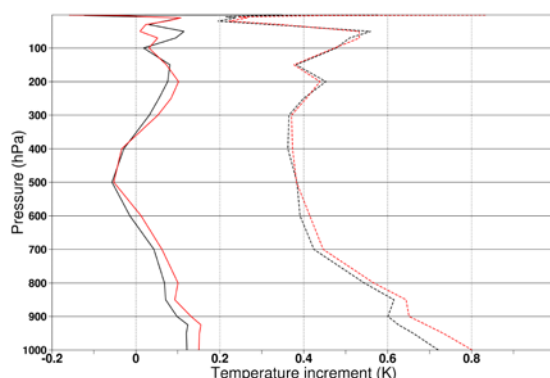


**Figure 3:** Mean and root-mean square temperature increments for a one month period. Solid lines indicate mean increments whereas dashed lines indicate root-mean square increments. Results for the IASI band 1 radiance assimilation experiment are in black whereas results for the IASI band 3 principal component assimilation experiment are in red.

The mean and random increments are changed everywhere (except a few narrow regions in the stratosphere and in the middle troposphere) by the use of IASI PC scores. The assimilation of IASI PC scores has the effect of systematically warming the analysis. Because the amplitude of the signal is very small, it is difficult to investigate the origin of these increments. One of the possibilities is that there are still residual biases in the PC scores that are not corrected the VarBC scheme. Regarding the larger random increments, we could argue that the IASI PC scores are working more than the long wave radiances in trying to correct errors in the temperature analysis. This hypothesis is not corroborated, however, by an improvement of the random fit to other types of observations.

In Figure 4 we show the bias and standard deviation of the departures between the temperature analysis/background and radiosonde observations. Results are shown for the B1 and B3\_OP\_PC experiment in the left and right panel respectively. In each panel, solid lines denote results for the background whereas dotted lines denote results for the analysis. The red curves refer to the actual experiment whereas the black curves always refer to the control experiment (i.e. the conventional data NOSAT experiment). The Northern Hemisphere is the geographical region north of 20 degrees latitude whereas the Southern Hemisphere is the geographical region south of -20 degrees latitude.

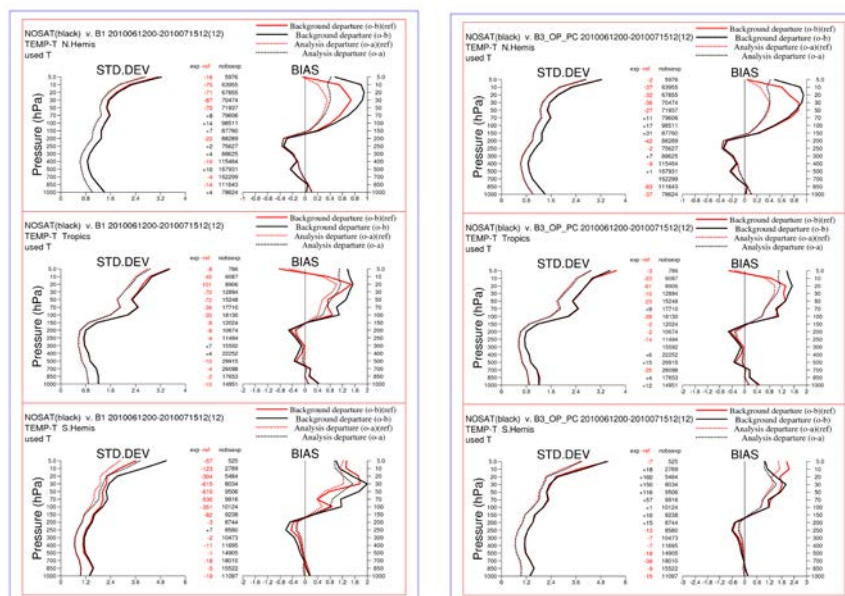


**Figure 4:** The verification against radiosondes of the background and analysis temperature profiles for: (left panel) the B1 experiment (red curve) and the NOSAT experiment (black curve), (right panel) the B3\_OP\_PC experiment (red curve) and the NOSAT experiment (black curve).

A comparison of the results for the B1 and B3\_OP\_PC experiments show some interesting features. When compared to the baseline NOSAT experiment (no satellite data) the assimilation of PC scores from IASI band 3 (B3\_OP\_PC experiment) improves the mean fit to radiosonde observations in the upper stratosphere and in the middle troposphere at tropical latitudes. There is also an improvement of the mean fit to radiosonde observations in the upper stratosphere in the extratropical Northern Hemisphere. In the same geographical region we also observe a slight improvement of the mean fit in the middle troposphere. In the extratropical Southern Hemisphere there is a very slight improvement of the mean fit to radiosonde observations in the middle troposphere. At these latitudes the PC score experiment degrades the fit to radiosondes in the upper stratosphere.

Results for the IASI long wave radiance experiment (B1) are in many respects similar with two notable exceptions. Firstly, when compared to the NOSAT experiment, the B1 experiment produces a sensible

improvement of the mean fit to radiosonde data between  $\approx 30$  and  $\approx 100$  hPa. This is not the case for the PC score experiment which does appear to have a very limited (if any at all) skill in this region of the atmosphere. Secondly, in the extratropical Southern Hemisphere, the improvement of the mean fit to radiosonde observations in the middle to lower troposphere is significantly larger for the B1 experiment. It should be noted, however, that in the lower troposphere below 700 hPa, the B1 experiment degrades the mean fit whereas the PC score experiment is basically neutral. The random fit to radiosonde observations does not appear to improve much when either long wave IASI radiances or IASI short wave PC score are used. Results are fairly neutral with the exception of the fit to stratospheric radiosondes in the extratropical Southern Hemisphere where the B1 system is greatly improving the fit whereas the B3\_OP\_PC system is typically neutral.

Regarding the behaviour of the PC score assimilation system between  $\approx 30$  and  $\approx 100$  hPa, at this stage we can only speculate that, as discussed in Section 2, it is probably related to the fact that in the coldest regions of the atmosphere short wave radiances are less sensitive than long wave radiances to temperature perturbations.

Results for the IASI short wave radiance assimilation system (B3\_OP) (not shown here) indicate that this system fails to replicate the results obtained by using the equivalent PC scores in the assimilation. There are in general no improvements over the NOSAT system with the exception of the random fit to radiosondes in the upper stratosphere in the extratropical Southern Hemisphere where the B3\_OP system gives a sensible improvement over the B3\_OP\_PC system. Because the B3\_OP system has not been fully tuned, we do not yet know if the overall better performance of the equivalent PC system is genuinely attributable to the intrinsic merits of PC analysis.

## 4.2 The Impact on Forecasts

We have run forecasts from the control and IASI assimilation systems. The forecasts have been verified using analyses for the period 10 June-12 July 2010. The forecast scores presented in this paper have been obtained by computing the difference between the root-mean-square forecast errors normalized by the forecast error in the experiment used as control. This is probably the best way to present the impact on forecast errors in the medium range but it also implies that small differences in the short range can be greatly amplified. At the same time, it has the advantage, over un-normalized plots, to dampen statistically insignificant signal that may appear on longer time-scales.

Figure 5 shows a cross-section of the root-mean-square forecast error differences for geopotential for the 120 hour forecasts. In the left panel we show results for the IASI long wave radiance assimilation system while in the right panel we show results for the IASI short wave PC score assimilation system. The control experiment is the conventional data assimilation system (NOSAT). The forecasts are verified against their own analyses. In all forecast plots shown in this paper, negative numbers indicate that either the inclusion of IASI radiances or PC scores is improving the forecast. The broad features of the forecast error differences for the two experiments are very similar. Results show that the largest forecast improvements are concentrated in the Southern Hemisphere where the B1 experiment seems to have a larger impact. We should stress, however, that the forecast improvements from the use of IASI PC scores are also significant. This is not the case for latitudes lower than 70 degree south where the use of IASI PC scores seems to have a decidedly negative impact on the forecast. In the remaining geographical region, results are comparable in magnitude although in some isolated regions the B1 experiment shows slight improvements not seen in the PC score experiment.

Finally, figures 6, 7, and 8, show the difference in normalized root-mean-square 500 hPa geopotential forecast error between the IASI and control systems for the extratropical Northern Hemisphere, the Tropical region, and, the extratropical Southern Hemisphere respectively. In each plot, the left panel depicts results for IASI long wave experiment while the right panel depicts results for IASI PC score experiment. The forecast is verified against the operational analysis, which contains information from IASI long wave radiances. Because short-range (i.e. one to three days) forecast errors are very sensitive to the dataset that is used to verify the forecast, they might not be indicative of the actual forecast skill. In the extratropical Northern Hemisphere the forecast impact is fairly neutral for both IASI experiments. In the tropical region, both experiments have a positive impact after day 2 with the IASI PC score experiment appearing slightly more significant in statistical terms. In the extratropical

Southern Hemisphere, both experiments show significant improvements although the impact of the IASI long wave experiment in the medium range is decidedly larger than the impact of the PC score experiment.

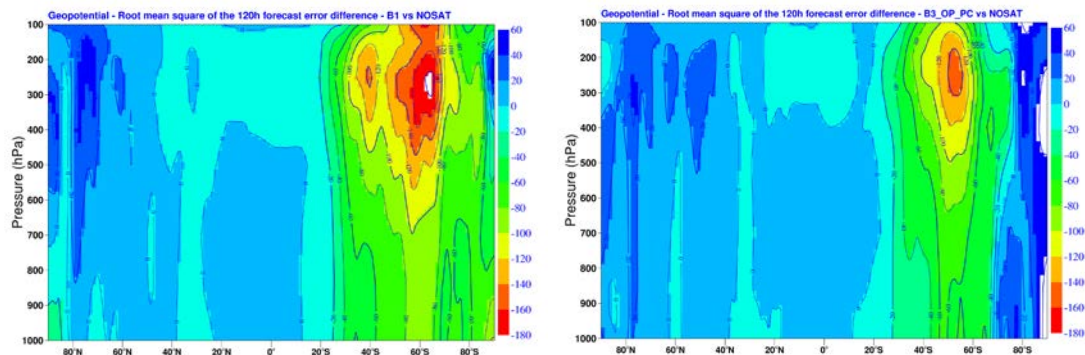


**Figure 5:** Cross-section of the root-mean-square forecast error difference in geopotential for 120 hour forecasts on assimilating (left panel) IASI band 1 radiances (experiment ECMWF\_B1), (right panel) IASI band 3 principal components (experiment ECMWF\_B3\_PC). Negative values indicate an improvement in forecast skill whereas positive values indicate a degradation in forecast skill. The forecasts are verified against their own analysis and are for the period 12 June 2010-10 July 2010.

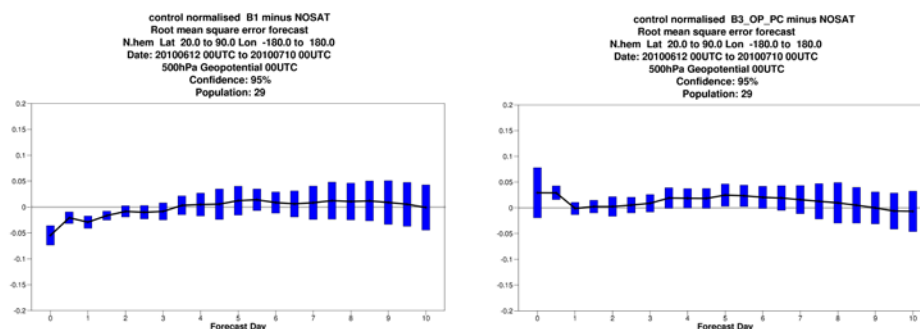


**Figure 6:** Northern hemisphere normalized root-mean-square error difference for 500 hPa geopotential forecasts for 12 June 2010-10 July 2010 verified versus the operational analysis. Positive values indicate a negative impact from the inclusion (left panel) of IASI band 1 radiances, (right panel) IASI band 3 principal components.

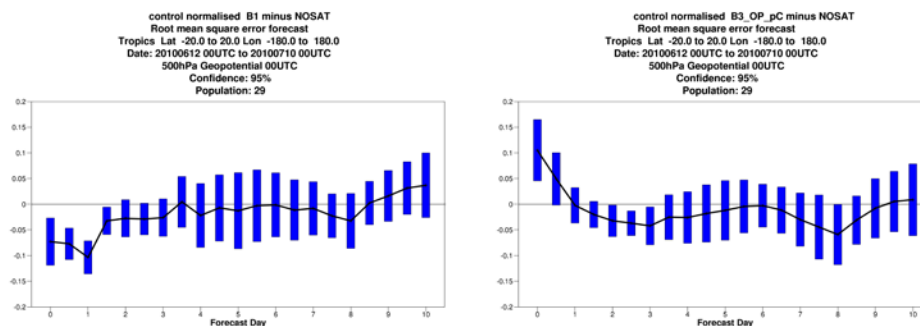


**Figure 7:** Tropical region normalized root-mean-square error difference for 500 hPa geopotential forecasts for 12 June 2010-10 July 2010 verified versus the operational analysis. Positive values indicate a negative impact from the inclusion (left panel) of IASI band 1 radiances, (right panel) IASI band 3 principal components.

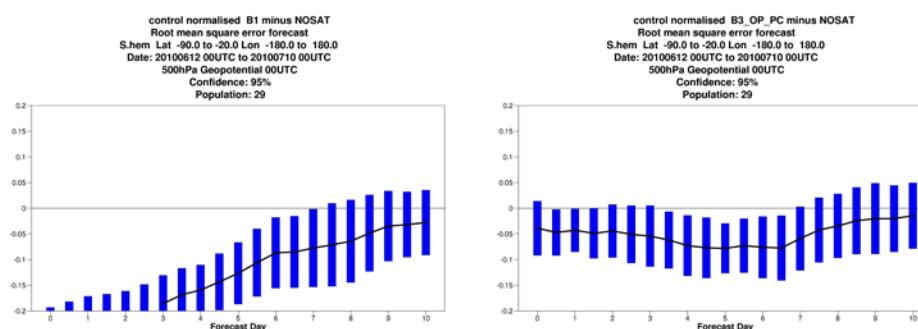


**Figure 8:** Southern hemisphere normalized root-mean-square error difference for 500 hPa geopotential forecasts for 12 June 2010-10 July 2010 verified versus the operational analysis. Positive values indicate a negative impact from the inclusion (left panel) of IASI band 1 radiances, (right panel) IASI band 3 principal components.

## 5 SUMMARY AND FUTURE WORK

The performance of an assimilation system based on the use of PC scores of IASI short wave radiances has been assessed by carrying out a series of four basic assimilation experiments. These experiments include a baseline experiment that uses only conventional data, a reference experiment that uses conventional data and the IASI operational long wave, a reference experiment that uses conventional data and 297 short wave IASI radiances, and, finally, a PC score experiment that uses conventional data and PC scores derived from 297 IASI short wave radiances. All experiments have been run during night-time to avoid any contamination due to solar radiation or non-LTE effects.

Results obtained in terms of forecast scores and radiosonde verification of background and analysis profiles are extremely significant and encouraging. In most cases, the PC score assimilation system (which is still in the early development stage) produces results that are very close to those produced by the more mature long wave radiance assimilation system. This should not, however, hide the fact that in data sparse regions like the extratropical Southern Hemisphere, we expect use of satellite data in the form PC scores to have a stronger impact. We should note, however, that the use of PC scores has a larger impact than the use of the corresponding short wave radiances although this results in not conclusive due to the very basic specification of the observation error in the short wave radiance experiment which we plan to revise any time soon.

Areas that could be further explored to better understand and improve the performance of the PC assimilation system include the refinement of the assumed observation errors, the cloud detection algorithm (and associated PC based quality control) and the bias correction scheme. When the performance of the PC assimilation has been optimized for clear sky conditions we will then be in a position to consider if the assimilation of IASI PCs can replace (or at least augment) the current use of IASI radiances in ECMWF operations.

## 6 REFERENCES

Antonelli P, Revercomb HE, Sromovsky LA, Smith WL, Knuteson RO, Tobin DC, Garcia RK, Howell HB, Huang H-L, Best FA. 2004. A principal component noise filter for high spectral resolution infrared measurements. *Journal of Geophysical Research*, Volume **109**, 2004, Doi:1029/2003JD004862.

Collard AD, McNally AP. 2009. Assimilation of IASI radiances at ECMWF, *Q. J. Roy. Meteorol. Soc.*, **135**: 1044-1058.



Dee D. 2004. Variational bias correction of radiance data in the ECMWF system. Proceedings of the ECMWF workshop on assimilation of high spectral resolution sounders in NWP, 28 June-1 July 2004, Reading, UK.

Kaplan L D, Chahine MT, Susskind J, Searl JE. 1977. Spectral band passes for a high precision satellite sounder. *Appl. Opt.* **16**, 322-325.

Matricardi M. 2010. A principal component based version of the RTTOV fast radiative transfer model. *Q.J. Roy. Meteorol. Soc.*, **136**, pp. 1823-1835.

Matricardi M, McNally T. 2011. The direct assimilation of IASI short wave principal component scores into the ECMWF NWP model. EUMETSAT Contract No. EUM/CO/07/460000475/PS.